

## Geometric approach in numerical eigenproblem analysis

Alexis Fedoroff and Reijo Kouhia

**Summary.** Non-linear eigenproblems can be encountered in a wide range of physical systems, stability analysis being an important source of such problems. The current technique used in commercial finite element codes to solve non-linear eigenproblems consists in linearizing the criticality equation with respect to the bifurcation parameter evaluated at the origin. Since the numerical technique is approximative, it is essential to assess the error both on the eigenvalue and the eigenmode. The latter one is of particular importance, since the eigenmode is typically used as initial imperfection in imperfection sensitivity analysis.

In this paper the authors propose a new geometric approach, in which the eigenvector is considered as a locally smooth function defined on the criticality manifold. Given two such eigenvectors, one for the non-linear eigenproblem and one for the linear one, it is possible to evaluate the error between the two eigenvectors considering the location of their respective arguments on the criticality manifold and the intrinsic properties of the criticality manifold itself. Simple, illustrative examples taken from structural stability will be shown for the sake of clarity as well as numerical computations on engineering problems.

*Key words:* non-linear eigenproblems, Riemannian geometry, structural stability

### Introduction

If we look at the role of engineers in the assessment of structural integrity for a given system it is rather clear that in order to avoid catastrophic events, emphasis should be placed on the study of qualitative changes in system behavior. From a theoretical point of view such qualitative changes in system behavior have been widely studied in the context of bifurcation theory [8], [23], [14], but as systems get more and more complex, numerical issues related to locating bifurcation points have to be taken into consideration. In the numerical study of non-linear phenomena eigenproblems play a significant role as a means of locating bifurcation points.

### *Numerical eigenproblem solution strategies*

Actually there are many different numerical strategies that have been developed over the years related to non-linear eigenproblem solving, and broadly we can conceive three types of approaches: indirect, direct and polynomial approximation approaches. The indirect approach consists in following the primary equilibrium path using continuation while monitoring some test function related to the criticality condition [21], [1], [3], [20], [12],[13]. Although continuation methods and their implementations in finite element codes tend to be reliable, these approaches need some experience from the user in order to properly set step length and other continuation parameters and certainly it is a time consuming approach. The direct approach consists in solving iteratively an augmented system consisting of equilibrium, criticality and normalization condition [10], [22], [18],

[26], [16]. The main issue in this approach is to find a suitable starting point within the radius of convergence of the iterative solver. Usually the starting point is found using the indirect strategy, which means that its drawbacks are also inherited. Although the direct approach has been widely discussed in the scientific literature, it has not yet found its way into commercial finite element codes. Instead of that the solution strategy proposed by most finite element codes to solve a non-linear eigenproblem seems to be the linear approximation of the eigenproblem with respect to the critical parameter evaluated at the origin.

Maybe because it has been seen as an engineering method, maybe because of its apparent simplicity, the linear approximation of the eigenproblem, as a numerical method, has not deserved much attention from the scientific community. The method itself dates back to the early days of finite element computation due to Gallagher [7], [19], and nowadays it is considered as standard textbook material [4], [5]. References can also be found in various finite element software manuals [2], which use either a tangent stiffness matrix approach or a secant stiffness matrix approach, although both variants can be considered as linearizations of a non-linear eigenproblem. An interesting study done by Earls [6] compares, for some benchmark structures, the critical values of linearized eigenproblem given by various finite element software packages with the analytic one. Although very recent studies using the linearized eigenproblem as part of a larger scope have been conducted [24, 17], as far as we know, there have been no publications on a priori error assessment of the linearized eigenproblem, either for the eigenvalue or the eigenmode.

### *The particular importance of eigenmode error assessment*

The reasons to study the a priori errors of a linearized eigenproblem are quite obvious. Linear approximation of an eigenproblem has the advantage of being fast and robust, and hence it is very popular among finite element software users. Maybe one reason for such popularity of linearized eigenproblem as a strategy is that it does not need any fine tuning from the user side, such as step length control or other parameter setting. In a design environment where the commercial finite element code is used as a “black box” by a user novice in numerical computation this point could be viewed as an important asset. However, as we will see in this article, the interpretation of the results given by a linear approximation of a non-linear eigenproblem is far from being trivial.

Therefore raises the question how accurate the solution of a linearized eigenproblem could possibly be, in other words what is the error of a given eigenpair with respect to a reference result obtained, for example, by a direct strategy. If we are solving a problem which could be qualified as quasi-linear with respect to the critical parameter, intuitively we would expect a good approximation obtained from the linearized problem both for the eigenvalue and the eigenmode. On the other hand, if we are considering “highly” non-linear systems, computational engineering practice assumes -falsely- that although the eigenvalue approximation could be bad, linearized eigenproblem yields always an acceptable approximation for the eigenmode. Instructive counterexamples using very simple structures will be given in section .

What then makes the error on *eigenmode* so significant over the error on *eigenvalue*? To answer to this question one needs to understand the standard stability analysis procedure used in structural engineering. Stability analysis of a structure starts by the eigenvalue analysis of a *geometrically perfect* structure using linearized buckling analysis.

In the resulting spectrum the most interesting eigenpair is obviously the most critical one, that is the one corresponding to the lowest positive eigenvalue. Now, the second part in stability analysis consists in introducing the eigenmode corresponding to the lowest positive eigenvalue as an initial imperfection and running a full non-linear analysis on the *geometrically imperfect* structure using a standard continuation method. Assuming that the post-critical path of the system under analysis is unstable, then one can find a limit point in the equilibrium path of the geometrically imperfect structure, which corresponds to the maximum load carrying capacity of the engineering problem. By experience the maximum load that the geometrically imperfect structure can bear is usually significantly lower than the buckling load given by the geometrically perfect system using non-linear eigenvalue analysis [11].

Now if we go through the standard stability analysis procedure we can see that the linearized eigenvalue is actually never used in structural integrity assessment. On the other hand when we carry out imperfection analysis the limit load that the geometrically imperfect structure can bear *depends* on the eigenmode obtained from the linearized eigenproblem, hence the emphasis on the role of the error on eigenmode.

### *Differential geometry and eigenproblem analysis*

In the present article we try to find some elements of an answer to characterize *a priori* the error of the linearized eigenmode. The sense of the word *a priori* here can be interpreted as “without knowing the result of the non-linear eigenproblem”. To be able to answer the question we have to find some generic properties which could possibly predict the change in the eigenmode as the matrix entries of the singular matrix, which defines the criticality condition, undergo a smooth change. It will be shown that the set of singular matrices constitutes a manifold embedded in the space of all square matrices and that the eigenvector is a locally smooth vector field on that singularity manifold. Further, we shall investigate the intrinsic properties of the singularity manifold, such as curvature, and try to relate it to a possible drastic change in the corresponding eigenmode. As far as we know, such an attempt to assess spectral properties of a linear operator using differential geometry approach is new and it seems very promising. Although in this article we shall mainly give results that have been constructed in the special case of two by two symmetric matrices, we are looking forward to generalize the results to arbitrary dimensions.

### **Overview on computational stability analysis**

As it already was mentioned, stability analysis is not just a single task, but rather a sequence of tasks that may vary depending on the nature of the problem under consideration. The type of stability problems most often encountered in stability analysis would be what singularity theorists would call *fold* and *cusp* bifurcations<sup>1</sup> [25, 8] which can be represented by the physical examples of snap-through and buckling, respectively. Another important point to consider is whether, in case of a cusp bifurcation, the post critical path is stable or unstable. That point is particularly important since it conditions the imperfection sensitivity of the system, and is a key issue when one has to decide whether to perform or not an imperfection sensitivity analysis. It should also be noted that a fold bifurcation is not imperfection sensitive.

<sup>1</sup>A bifurcation is a point on the equilibrium path where the number of solutions to the equilibrium equation changes as the critical parameter varies [8]

In the following few sections we shall describe very briefly the different stages that the stability analysis of conservative systems could possibly consist of, without, however going into the details of postbuckling analysis and imperfection sensitivity analysis, as these topics are out of the scope of this article. We shall also set forth the specific problematics related to non-linear eigenproblem analysis as opposite to linearized eigenproblem analysis and try to compare the results in terms of eigenvalues and eigenmodes.

### *Defining the equilibrium path*

Assume that for a conservative system the potential energy functional  $\Pi \in \mathcal{C}^k(X \times \mathbb{R}; \mathbb{R})$  is available and it is smooth, and where  $X$  denotes some Hilbert space called the state space, which for discrete systems is the euclidean space  $\mathbb{R}^n$  endowed with the 2-norm. In a static loading case one can assume that a conservative system is at equilibrium if the first variation of the potential energy vanishes. One can then compute the defining function  $\mathbf{f} \in \mathcal{C}^k(X \times \mathbb{R}; X)$  of the equilibrium equation from the relation  $\delta\Pi|_{(\mathbf{p}, \lambda)}(\mathbf{q}) = \langle \mathbf{q}, \mathbf{f}(\mathbf{p}, \lambda) \rangle$ , where  $\mathbf{p}$  is an element in the state space  $X$ ,  $\mathbf{q}$  a vector in the tangent space  $T_{\mathbf{p}}X$ , and  $\langle \cdot, \cdot \rangle$  denotes the inner product in  $X$ . Note that since we assume  $X$  to be euclidean, the tangent space  $T_{\mathbf{p}}X$  can be assimilated to the state space  $X$  itself. The critical parameter  $\lambda$  is a real-valued quantity on which the equilibrium state depends. The zero set of the defining function  $\mathcal{E} := \{(\mathbf{p}, \lambda) \in X \times \mathbb{R} : \mathbf{f}(\mathbf{p}, \lambda) = 0\}$  can then be viewed as the equilibrium path. The equilibrium path is made up of one or more branches  $\mathcal{E}_i$ ,  $i \in \mathbb{N}$  such as the set union of all branches makes up the whole equilibrium path, and it can be shown that each branch is a smooth 1-manifold embedded in the ambient state space [9]. The branch which contains the origin of the state space, i.e. the point corresponding to the reference configuration is called the primary branch or primary equilibrium path and is noted  $\mathcal{E}_1$ .

### *Defining the jacobian mapping and finding the critical points*

The next step in classical stability analysis consists in the investigation of critical points, which in turn enables to assess the quality of the equilibrium path. The Lagrange-Dirichlet stability criterion, which is usually the most appropriate one in a static loading scheme, tells that the equilibrium of a conservative system is locally stable if and only if the potential energy functional has a local minimum. As a corollary one can retain that a point on the equilibrium path is stable if the second variation of the potential energy functional is positive definite in all possible directions.

Since we are primarily interested in the points where the equilibrium path quality changes from stable to unstable, we shall use the criticality condition, also called the Trefftz condition, to find those points. The second variation of the potential energy functional is related to the jacobian of the defining function in the following way:  $\delta^2\Pi|_{(\mathbf{p}, \lambda)}(\mathbf{q}, \mathbf{q}) = \langle \mathbf{q}, \mathbf{J}|_{(\mathbf{p}, \lambda)} \mathbf{q} \rangle$ , where we have used the notation  $\mathbf{J} := \partial_{\mathbf{p}}\mathbf{f}$  to denote the jacobian matrix mapping from the equilibrium set to the set of bounded linear operators:  $\mathbf{J} \in \mathcal{C}^k(\mathcal{E}; \text{BL}(X; X))$ . If we consider the restriction of  $\mathbf{J}$  to a given branch  $\mathcal{E}_i$ , then the range of that restricted mapping also constitutes a 1-manifold  $\mathcal{J}_i$  embedded in the ambient space of bounded linear operators  $\text{BL}(X; X)$ . Note that in case of discrete systems the ambient space just the set of square  $n \times n$  matrices.

At a critical point  $(\hat{\mathbf{p}}, \hat{\lambda})$  belonging to the equilibrium path  $\mathcal{E}$  we may assume that there exists at least one direction in the state space noted  $\hat{\mathbf{q}}$  such as the quantity  $\mathbf{J}|_{(\hat{\mathbf{p}}, \hat{\lambda})} \hat{\mathbf{q}}$

vanishes. It is easy to see then that if we consider a chart<sup>2</sup>  $(\psi, V)$  of  $\mathcal{E}_i$ , then the mapping  $\mathbf{J} \circ \psi^{-1} \in \mathcal{C}^k(\psi(V); \mathcal{J}_i)$  defines a non-linear eigenvalue problem  $(\mathbf{J} \circ \psi^{-1})|_{\hat{t}} \hat{\mathbf{q}} = 0$  such that  $\hat{t} = \psi(\hat{\mathbf{p}}, \hat{\lambda})$ .

### *Defining the linear approximation of the eigenproblem*

With some experience, one can easily notice that finding analytical solutions is difficult even in extremely simple cases. For more complex systems it can be assumed that global analytical solutions are unavailable, hence the only way to proceed with stability analysis consists in finding numerical solutions to the non-linear eigenproblem. Numerical solutions can be “exact” in the sense that there is an Newton-like iterative algorithm that converges to the exact solution, or the numerical solution can be “approximative” in the sense that an approximative solution is found using Taylor-like local formulas that are easy to solve.

Let us find out what happens if we apply a Taylor series expansion to the equilibrium and criticality condition. First linearize at the origin the non-linear equilibrium defining function  $\mathbf{f}$  with respect to the critical parameter  $\lambda$

$$\mathbf{f}(\mathbf{p}, \lambda) = \mathbf{f}|_{(\mathbf{o},0)} + \left( \partial_{\mathbf{p}} \mathbf{f}|_{(\mathbf{o},0)} \left( \frac{d\mathbf{p}}{d\lambda} \Big|_0 \right) + \partial_{\lambda} \mathbf{f}|_{(\mathbf{o},0)} \right) \lambda + \mathcal{O}(\lambda^2). \quad (1)$$

Since the equilibrium relation  $\mathbf{f}(\mathbf{p}, \lambda) = 0$  has to hold for any value of  $\lambda$  it may be inferred that each coefficient of the polynomial in  $\lambda$  given by the right hand side of equation (1) has to be equal to zero. Hence the derivative of the state variable  $\mathbf{p}$  with respect to the critical parameter  $\lambda$  can be evaluated provided that the jacobian  $\partial_{\mathbf{p}} \mathbf{f}$  evaluated at the origin is not singular:  $\frac{d\mathbf{p}}{d\lambda} \Big|_0 = - \partial_{\mathbf{p}} \mathbf{f}|_{(\mathbf{o},0)}^{-1} \mathbf{f}|_{(\mathbf{o},0)}$ . Using that value one can draw the linear equilibrium path tangent at the origin, which is just the graph of the function  $\lambda \mapsto \frac{d\mathbf{p}}{d\lambda} \Big|_0 \lambda$ . It is quite easy to prove that the linear equilibrium path is just the tangent space  $T_0 \mathcal{E}_1$  at the origin to the primary equilibrium path  $\mathcal{E}_1$ . Next, let us compute the linear approximation of the jacobian matrix:

$$\mathbf{J}|_{(\mathbf{p},\lambda)} = \mathbf{J}|_{(\mathbf{o},0)} + \left( \partial_{\mathbf{p}} \mathbf{J}|_{(\mathbf{o},0)} \left( \frac{d\mathbf{p}}{d\lambda} \Big|_0 \right) + \partial_{\lambda} \mathbf{J}|_{(\mathbf{o},0)} \right) \lambda + \mathcal{O}(\lambda^2). \quad (2)$$

Likewise, one can prove that the linearization of the jacobian mapping given by equation (2) defines a manifold embedded in the ambient space of bounded linear operators that actually is the tangent space  $T_0 \mathcal{J}_1$  to the manifold  $\mathcal{J}_1$ . The linearized criticality condition then yields the following generalized linear eigenvalue problem:  $\mathbf{J}|_{(\mathbf{o},0)} \hat{\mathbf{q}} = -\hat{\lambda} \left( \partial_{\mathbf{p}} \mathbf{J}|_{(\mathbf{o},0)} \left( \frac{d\mathbf{p}}{d\lambda} \Big|_0 \right) + \partial_{\lambda} \mathbf{J}|_{(\mathbf{o},0)} \right) \hat{\mathbf{q}}$ .

For practical consideration we are interested in the eigenpair corresponding to the minimum positive eigenvalue (assuming, of course, that there exists one and that it is unique). In the following sections of this article we shall denote by  $(\lambda^{\text{NL}}, \mathbf{q}^{\text{NL}})$  and  $(\lambda^{\text{LIN}}, \mathbf{q}^{\text{LIN}})$  the eigenpair solutions of the non-linear and linear eigenproblems respectively.

### **Examples and motivation**

In order to get a more palpable view of the problematics, to illustrate the research questions and to motivate the theoretical discussion that follows, let us start by investigating the stability of two very simple, idealized systems. The first system we want to analyze is

<sup>2</sup>In differential geometry a chart  $(\psi, V)$  is an ordered pair where  $\psi$  is a homeomorphism from an open subset  $V$  on the manifold to an open subset of the euclidean space [15].

a two degree of freedom model that models the snap-through behavior of a dome shaped structure. The second system tries to predict the out-of-plane buckling behavior of an initially plane truss. We have thus chosen two representatives of the fold and cusp bifurcations respectively. Both models are by no means perfect, however they present the invaluable asset of being analytically computable and behave in a way that is easy to understand intuitively. Nevertheless they are complex enough to exhibit the phenomena we are interested in.

### First example: snap-through of a dome

#### Defining the system

Consider the following two degree of freedom model, depicted in figure 1, that is supposed to represent a dome-shaped system with polar symmetry or an arch restricted to plane displacements. The dome or arch is assumed to have a finite and constant membrane stiffness and a negligible bending stiffness. From figure 1 one can see that the radial membrane stiffness is represented by the quantity  $\gamma k$  and the radial membrane stiffness is represented by the quantity  $\frac{1}{2} k$ . The non-dimensional factor  $\gamma$  relates the two quantities. The question of how well this simple model is representing a given physical system is of no importance, since the aim of this exercise is to show the problems related to approximative solutions that may arise in stability analysis. In the setup of kinematical relationships

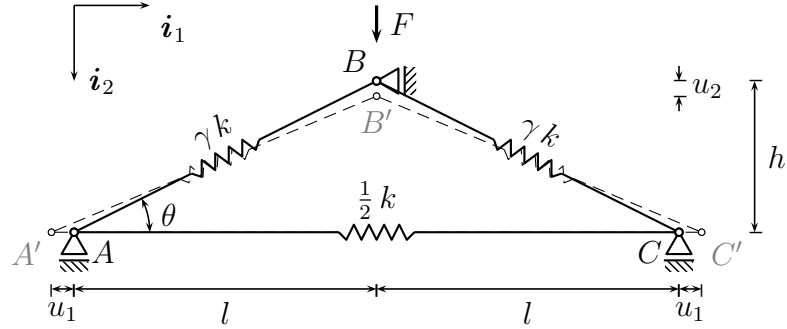


Figure 1. A mathematical model of the snap-through problem.

we shall make some arbitrary choices concerning the measure of strain, mainly guided by the pursue of simplicity. The choice of the strain measure is inspired from the Green-Lagrange strain tensor in such a way that it defines the strain for a given segment  $PQ$  in the reference configuration, denoted  $P'Q'$  in the deformed configuration by

$$\epsilon_{PQ} := \frac{1}{2} \frac{\|P'Q'\|^2 - \|PQ\|^2}{\|PQ\|^2}. \quad (3)$$

Further considering the vector decompositions  $A'B' = (l + u_1) \mathbf{i}_1 - (h - u_2) \mathbf{i}_2$ ,  $B'C' = (l + u_1) \mathbf{i}_1 + (h - u_2) \mathbf{i}_2$  and  $A'C' = 2(l + u_1) \mathbf{i}_1$  in the orthonormal basis  $\{\mathbf{i}_1, \mathbf{i}_2\}$ , the shorthand notation  $\|AB\| = \|BC\| =: d$ , and the non-dimensional state variables  $p_1$  and  $p_2$  defined as follows:  $p_1 := u_1/d$ ,  $p_2 := u_2/d$ , on ends with the following expressions of the strains:

$$\epsilon_{AB}(\mathbf{p}) = \frac{1}{2} \left( (\cos \theta + p_1)^2 + (\sin \theta - p_2)^2 - 1 \right) = \epsilon_{BC}(\mathbf{p}), \quad (4a)$$

$$\epsilon_{AC}(\mathbf{p}) = \frac{1}{2} \left( (\cos \theta + p_1)^2 / \cos^2 \theta - 1 \right). \quad (4b)$$

The potential energy of a linear elastic spring segment  $PQ$  can be expressed as half the product of the spring constant with the elongation of the spring. Hence one can easily find the potential energy of the example problem by summing the potential energies for each individual segment. Doing this with the non-dimensional quantities yields the following expression for the total potential energy functional:

$$\Pi(\mathbf{p}, \lambda) = \frac{1}{2} \gamma \epsilon_{AB}^2(\mathbf{p}) + \frac{1}{2} \cos^2 \theta \epsilon_{AC}^2(\mathbf{p}) - \lambda p_2 . \quad (5)$$

In the above equation the non-dimensional load parameter  $\lambda$  is defined as the following quantity  $\lambda := F/(2kd)$ .

For this particular example the equilibrium path  $\mathcal{E}$  can be calculated analytically quite easily from the equilibrium equations although we shall not go into details here, as it is not the purpose of this article. Just note that by making appropriate change of variable one can find out that the projection of the equilibrium path on the plane  $\{\lambda = 0\}$  is an ellipse and that the projection of the equilibrium path on the plane  $\{p_1 = 0\}$  is a cubic polynomial in  $p_2$ . Then by applying a polar parametrization one can easily draw the equilibrium path in the state space. As far as the critical points is concerned, they can be computed very neatly using the constants which corresponds to the major and minor axis of the ellipse.

#### *Presenting the results in the classical state space*

Let us present now the obtained results in the classical state space. In figures 2 and 3 we have shown the equilibrium path, which actually is the primary and only one  $\mathcal{E}_1$ . Also the tangent space at the origin, which represents the linearized equilibrium path, have been represented. Stable portions of the equilibrium path appear in black solid line whereas unstable portions in gray solid line. Further, the critical points and the eigenmodes computed from both the non-linear eigenproblem and the linearized one have been pictured in the state space.

One can see that for some parameter values, the relative error on the eigenvalue defined as  $(\lambda^{\text{NL}} - \lambda^{\text{LIN}})/\lambda^{\text{NL}}$  can be relatively large. On the other hand the error on the eigenmode, which is here defined to be the quantity  $1 - |\langle \mathbf{q}^{\text{NL}}, \mathbf{q}^{\text{LIN}} \rangle|$  is very small. If one scans though all possible physically meaningful values of the parameters  $\gamma$  and  $\theta$ , it can be observed that in *most* situations the error on the eigenmode remains very small, even though the error on the eigenvalue can be hundreds of percents. However the example given in figure 3 shows, that for some parameter values the relative error on the eigenmode can be important.

Looking at figures 2 and 3 one can see that there is clearly a particular point that the state space representation cannot explain, namely the direction of the linearized eigenmode. If we consider the non-linear eigenmode, it looks obvious from the figures that it is always an element of the tangent space at the critical point. However, one cannot say the same of the linearized eigenmode, which seems to point to an arbitrary direction. Therefore let us try another way of presenting the results, which -we hope- is more adequate.

#### *Presenting the results using the criticality manifold*

The crucial thing in understanding the following sections comes from the consideration of the set of all square  $n \times n$  real matrices as a vector space. Indeed, it can be shown

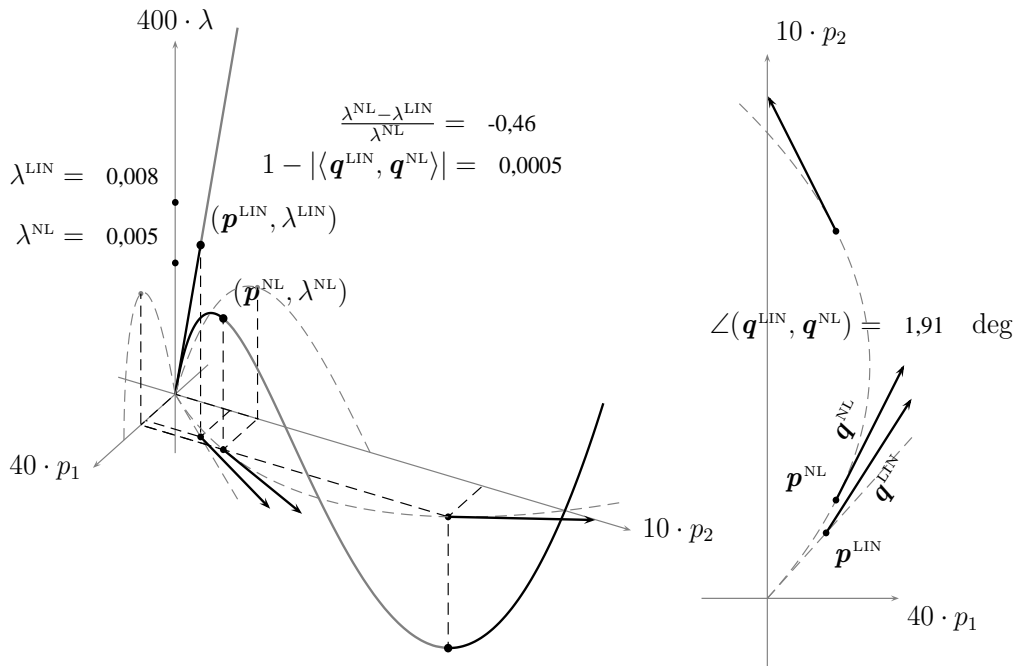


Figure 2. Equilibrium path for the example problem with parameter values  $\gamma = 2$  and  $\theta = 20$  deg

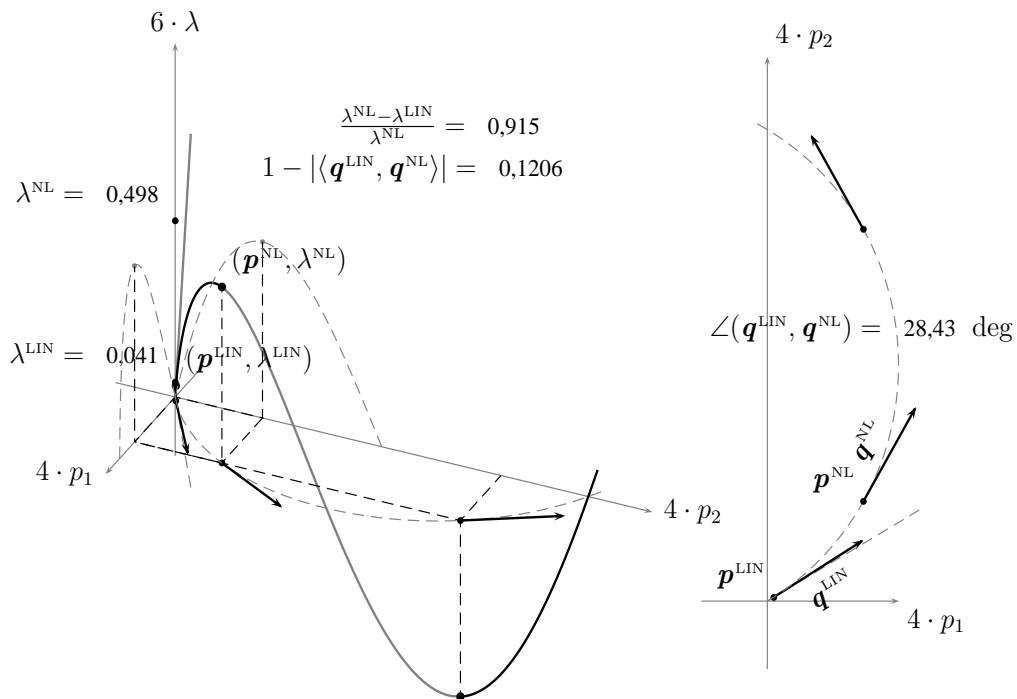


Figure 3. Equilibrium path for the snap-through example problem with parameter values  $\gamma = 1000$  and  $\theta = 60$  deg

that such set endowed with the addition and multiplication by an element in the field  $\mathbb{R}$  constitutes a vector space. We can also show that if we further endow the space  $\mathbb{R}^{n \times n}$  with an appropriate inner product, we can construct an orthonormal basis for that space  $\{\mathbf{e}_i \mathbf{e}_j^\top : 1 \leq i \leq n, 1 \leq j \leq n\}$ . For example the base vectors for the space  $\mathbb{R}^{2 \times 2}$  would be  $\mathbf{e}_1 \mathbf{e}_1^\top$ ,  $\mathbf{e}_1 \mathbf{e}_2^\top$ ,  $\mathbf{e}_2 \mathbf{e}_1^\top$  and  $\mathbf{e}_2 \mathbf{e}_2^\top$ . In the graphical interpretations that will come ahead we shall use analogy with the classical euclidean state space and draw the unit vectors

$\mathbf{e}_i \mathbf{e}_j^\top$  as arrows.

The criticality manifold is here defined as the set of all square  $n \times n$  real matrices of rank  $n - 1$  or less. It can be shown [15] that the set of all matrices of rank  $n - 1$  is a smooth manifold of dimension  $n^2 - 1$  embedded in  $\mathbb{R}^{n \times n}$  and that matrices of lower rank constitute submanifolds thereof. If we consider the special case of symmetric matrices, they form a  $n(n + 1) / 2$  dimensional ambient space and the criticality manifold would be  $n(n + 1) / 2 - 1$  dimensional. In the particular case of our example problem we have a 2-dimensional criticality manifold embedded in the space of symmetric  $2 \times 2$  matrices.

As we already stated, the range of the jacobian mapping restricted to a particular branch of the equilibrium path  $\mathbf{J} : \mathcal{E}_i \rightarrow \mathbb{R}^{n \times n}$  defines a 1-manifold  $\mathcal{J}_i$ , also embedded in the ambient space of square  $n \times n$  real matrices. We shall focus on the branch corresponding to the primary equilibrium path and shall call it the primary jacobian path,  $\mathcal{J}_1$ .

In figure 4 and 5 we have drawn both the criticality manifold and the primary (and only) jacobian branch of the non-linear problem as well as the jacobian branch of the linearized problem. Positive definite parts have been drawn in black solid line and indefinite portions in gray. The intersection points between the jacobian paths and the criticality manifold correspond to the solutions of the criticality condition. Note that if one uses a parametrization  $\varphi$  that consists in “wrapping” the criticality manifold with a sheet of paper without tearing or crumpling it, then for two given singular matrices  $\mathbf{A}$  and  $\mathbf{B}$  the angle between the corresponding eigenmodes  $\angle(\mathbf{q}_A, \mathbf{q}_B)$  depends only on the central angle  $\angle(\varphi(\mathbf{A}), \varphi(\mathbf{B}))$  between the points  $\varphi(\mathbf{A})$  and  $\varphi(\mathbf{B})$ . Moreover the dependence is linear with a factor of  $\sqrt{2}$ . We shall prove this claim in detail in subsequent sections, but this type of relation starts to look like what we are searching.

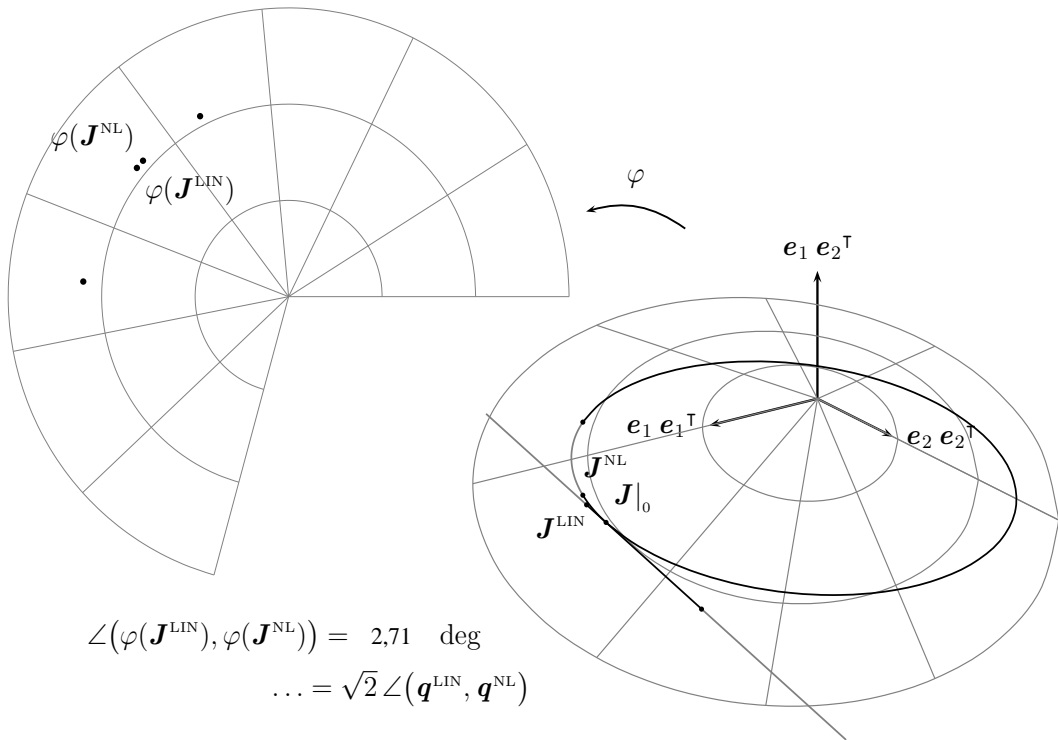


Figure 4. Jacobian path and criticality manifold for the snap-through example problem with parameter values  $\gamma = 2$  and  $\theta = 20 \text{ deg}$ .

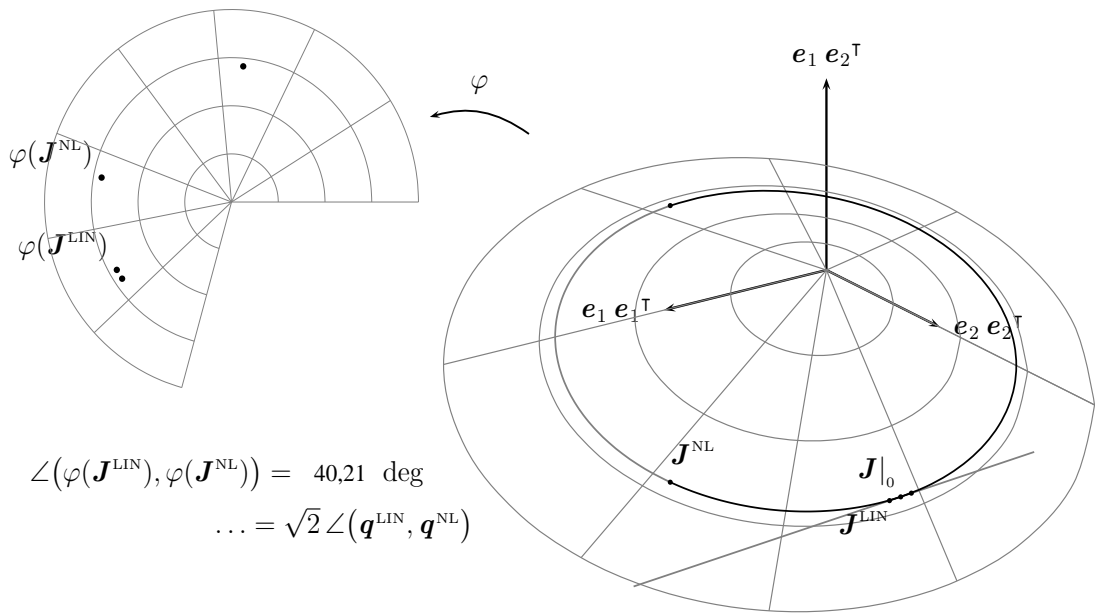


Figure 5. Jacobian path and criticality manifold for the snap-through example problem with parameter values  $\gamma = 1000$  and  $\theta = 60 \text{ deg}$

### Second example: out-of-plane buckling

#### Defining the system

Consider the following three degree of freedom model as shown in figure 6. Although it is not evident, this model is representing a truss structure that is initially plane with a loading constricted to that plane. The plane in question is the one orthogonal to  $\mathbf{e}_1$  going through the point  $A$ . Note that the point  $A'$  is always restricted to that plane, and that in the reference placement the point  $A$  coincides with the point  $O$ . The structure is able to buckle in two different modes, or combinations thereof: as a rigid bar, such that the segments  $A'B'$  and  $B'C'$  remain in line, or as euler column buckling such as the nodes  $A'$  and  $C'$  remain in the original plane while the “column” consisting of the rigid segments  $A'B'$  and  $B'C'$  “bends” at  $B'$ .

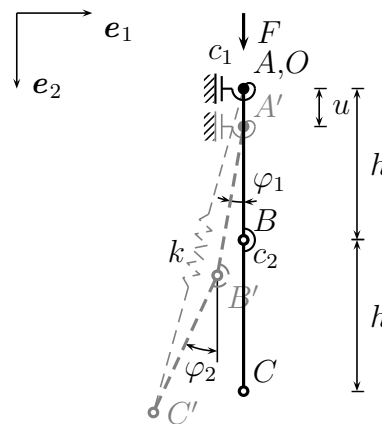


Figure 6. A mathematical model of the out-of-plane buckling problem

The point  $A'$  is connected to the rigid frame via a “torsional” linear spring with coefficient  $c_1$  whereas the relative angle of  $A'B'$  with respect to  $B'C'$  is controlled by a

“flexural” linear spring with coefficient  $c_2$ . The nodes  $O$  and  $C'$  are connected to each other via an axial linear spring of coefficient  $k$ . One can assume that the strain measure in the axial spring is given by a Green-Lagrange type measure as shown in equation (3). Consider the vector quantity  $OC' = -h(\sin \varphi_1 + \sin \varphi_2) \mathbf{e}_1 + (u + h(\cos \varphi_1 + \cos \varphi_2)) \mathbf{e}_2$  and the non-dimensional state variables  $p_1 := u / (2h)$ ,  $p_2 := (\varphi_2 + \varphi_1)/2$  and  $p_3 := (\varphi_2 - \varphi_1)/2$  as well as the constants  $\eta_1 := c_1 / (k(2h)^2)$ ,  $\eta_2 := 4c_2 / (k(2h)^2)$  and  $\lambda := F / (k2h)$ . Then, considering the following expression for the strain measure,

$$\epsilon_{OC}(\mathbf{p}) = \frac{1}{2} \left( 2p_1 \cos p_2 \cos p_3 + \cos^2 p_3 + p_1^2 - 1 \right), \quad (6)$$

one can build the following non-dimensional expression for the total potential energy functional:

$$\Pi(\mathbf{p}, \lambda) = \frac{1}{2} \epsilon_{OC}^2(\mathbf{p}) + \frac{1}{2} \eta_1 (p_2 - p_3)^2 + \frac{1}{2} \eta_2 (p_3)^2 - \lambda p_1. \quad (7)$$

Although we shall not go into the details of computing the equilibrium paths and critical points of this system, we feel that the reader who might want to compute the analytical solutions should be informed that the graphical representations given in the following sections have been computed in exchange for a somewhat arbitrary simplification. Namely the second order term  $p_1^2$  in the strain measure expression (6) has been neglected, and the reasons to that are quite opportunistic. As a matter of fact, we wanted to show a case where even assuming a linear primary equilibrium path the events with respect to eigenproblem linearization could well be pathological.

#### *Presenting the results in the classical state space*

Figure 7 shows the equilibrium paths projected on the hyperplanes  $\{p_2 = 0, p_3 = 0\}$  and  $\{\lambda = 0\}$ . The example has been calculated for a particular case where the ratio of  $\eta_2$  to  $\eta_1$  is 20, meaning that the torsional rigidity  $c_1$  of the upper chord of the truss is only 1/5 of the flexural rigidity  $c_2$  of the compressed vertical member.

As we already mentioned, due to the simplification we managed to get a linear primary path although the real primary path according to the accurate mathematical model up to the critical points would probably have been very close to linear. Nevertheless this is not our primary cause of concern. Looking at the secondary equilibrium paths, one can clearly see that at the lower positive critical point given by the non-linear eigenproblem the eigenmode is pointing almost in the direction of  $p_2$ , i.e.  $\varphi_1 \approx \varphi_2$ , suggesting a rigid bar buckling mode. On the other hand the higher positive critical point given by the non-linear eigenproblem suggests, by pointing almost at  $p_3$ , a euler column buckling mode ( $\varphi_1 \approx -\varphi_2$ ).

Then, if we look at the result given by the linearized eigenproblem, it seems to point in the direction such that  $p_2 \approx p_3$ , which means that  $\varphi_2 \approx 0$ . Physically this eigenmode is rather unexpected considering the values that have been given to the spring constants.

#### *Presenting the results using the criticality manifold*

Let's have a look at the results how they appear on the criticality manifold and then discuss what possible benefits one could get from this type of representation. Figure 8 shows the primary jacobian path  $\mathcal{J}_I$  embedded in the ambient  $\mathbb{R}^{3 \times 3}$  space of symmetric square matrices. However, since the jacobian matrix evaluated at the primary path of equilibrium is block diagonal and that the block related to the primary state variable  $p_1$  is assumed to be non-singular (it is actually constant in this case), we shall investigate the

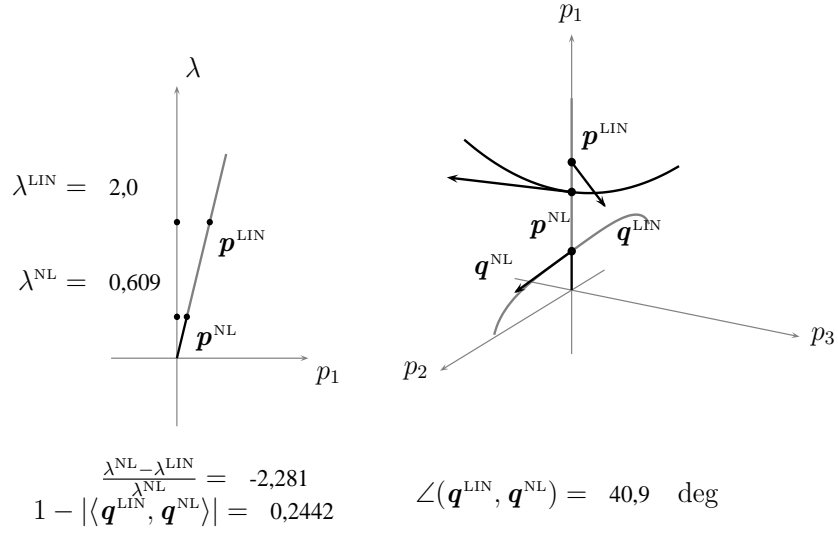


Figure 7. Equilibrium path for the out-of-plane buckling example problem with parameter values  $\eta_1 = 0.1$  and  $\eta_2 = 2.0$

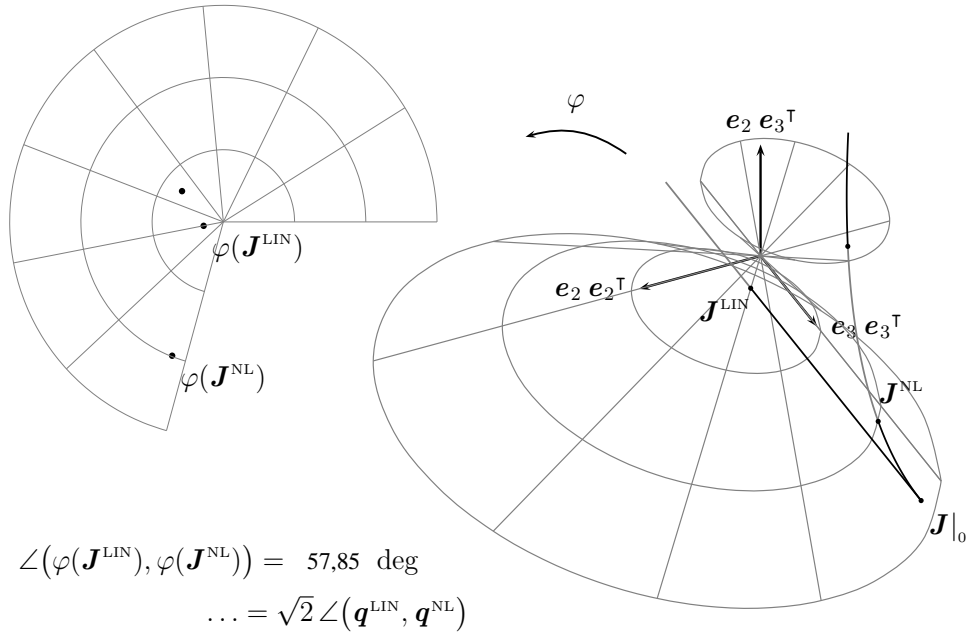


Figure 8. Jacobian path and criticality manifold for the out-of-plane buckling example problem with parameter values  $\eta_1 = 0.1$  and  $\eta_2 = 2.0$

positive definiteness only of the block related to the secondary state variables  $p_2$  and  $p_3$ . Since we are dealing with symmetric matrices, it is easy to draw the criticality manifold and the primary jacobian paths projected on the space spanned by  $\{\mathbf{e}_2 \mathbf{e}_2^\top, \mathbf{e}_3 \mathbf{e}_3^\top, \mathbf{e}_2 \mathbf{e}_3^\top\}$ .

From figure 8 it is easy to see that although the primary equilibrium path  $\mathcal{E}_1$  is linear, the primary jacobian path  $\mathcal{J}_1$  is far from being linear. One can further notice that both the non-linear jacobian path  $\mathcal{J}_1$  and the tangent space  $T_0 \mathcal{J}_1$  are fully contained in the plane  $\{[\mathbf{J}]_{23} = -\eta_1\}$  and that the tangent space is parallel to the vector  $\mathbf{e}_3 \mathbf{e}_3^\top$  in the

matrix space. The latter statement implies that there is only one intersection between the criticality manifold and the tangent space.

### **Differential geometry approach in two dimensional symmetric eigenproblems**

Let's now try to produce some kind of theory around the questions that have been sketched in the examples and motivation section. Knowing that a general theory valid in a Hilbert space or even a theory valid for discrete systems involving eigenproblems in the  $n \times n$  ambient matrix space would be too a big leap forward in a first approach, we shall restrict ourselves to the very modest case of symmetric  $2 \times 2$  matrix space in this article. The first reason is that the geometrical objects occurring in these spaces are fairly well known for most of the readers, since we are going to manipulate something very similar to surfaces embedded in the three dimensional euclidean space. The second reason is that we need at least two dimensions in order to make a difference between two eigenvectors, so the space we are considering is the simplest one that could possibly give answers to our questions.

As we have seen from the previous examples, trying to make some general statements about the jacobian path of a generic physical system can prove to be very difficult. In both examples that we have considered so far the jacobian path was a plane curve, and the tangent space to the jacobian path obviously lies then in the same plane. However in a generic case we have to consider a jacobian path as an arbitrary curve in the ambient space. Furthermore, one can intuitively see that although the error on the eigenvalue depends on the distance travelled from the origin all the way to the critical point along the non-linear and the linearized jacobian paths respectively, the error on the eigenmode depends only on the respective positions of the non-linear and linearized critical points on the criticality manifold.

Therefore in this general approach we shall forget about the jacobian paths altogether and focus solely on the properties on the criticality manifolds and how they affect the corresponding eigenmodes. We shall consider therefore the eigenmode as a locally smooth mapping from the criticality manifold to the state space. This claim is proved below in lemma 1. The next step is to compute the error between two eigenmodes and to show that this is also a smooth mapping on the criticality manifold. The next step constitutes in finding a proper parametrization as a collection of charts on the criticality manifold such that one can easily define and recognize geodesics on the manifold. Geodesics can loosely be understood as shortest ways on a manifold between two points. Finally, the last step consists in explicitly computing the error between the eigenmode as a function of some intrinsic properties of the criticality manifold and the distance between the two points under consideration.

Since our goal is to make some a priori statement on the error on the eigenmode we do not have any reference point at our disposal. Therefore we have to consider an open ball of some radius  $\epsilon$  around a given point on the criticality manifold and try to estimate the error on the eigenmode as a function of the radius  $\epsilon$  and the intrinsic properties of the manifold at the point under consideration.

#### *Properties of the eigenmode and error on eigenmode mappings*

Consider the criticality manifold defined as the set of all square  $n \times n$  matrices of rank  $n - 1$  with real entries. It can be shown that this set constitutes a smooth manifold [15] that we shall denote  $\mathcal{M}_1^n$ .

**Lemma 1** (Local smoothness of the eigenmode mapping). *Consider a smooth manifold  $\mathcal{M}_1^n$ . Then  $\mathbf{q} : \mathcal{M}_1^n \rightarrow \mathbb{R}^n$  defined by the map  $\mathbf{A} \mapsto \mathbf{q}_A$  such that  $\mathbf{A} \mathbf{q}_A = 0$  and  $\|\mathbf{q}_A\| = 1$  is a locally smooth map on  $\mathcal{M}_1^n$ .*

*Proof.* For any matrix  $\mathbf{A} \in \mathcal{M}_1^n$ , there exists a permutation matrix  $\mathbf{P} \in \mathbb{R}^{n \times n}$  such as

$$\mathbf{P}^\top \mathbf{A} \mathbf{P} = \begin{pmatrix} \mathbf{M} & \mathbf{m} \\ \mathbf{n}^\top & \mathbf{n}^\top \mathbf{M}^{-1} \mathbf{m} \end{pmatrix} \quad (8)$$

where the matrix  $\mathbf{M} \in \mathbb{R}^{(n-1) \times (n-1)}$  is full rank,  $\mathbf{m} \in \mathbb{R}^{(n-1) \times 1}$  and  $\mathbf{n}^\top \in \mathbb{R}^{1 \times (n-1)}$ . The right hand side matrix is obviously rank  $n - 1$ , since it can be decomposed as a product of a full rank matrix and a matrix with the last row of zeros:

$$\begin{pmatrix} \mathbf{M} & \mathbf{m} \\ \mathbf{n}^\top & \mathbf{n}^\top \mathbf{M}^{-1} \mathbf{m} \end{pmatrix} = \begin{pmatrix} \mathbf{I} & 0 \\ \mathbf{n}^\top \mathbf{M}^{-1} & 1 \end{pmatrix} \begin{pmatrix} \mathbf{M} & \mathbf{m} \\ 0 & 0 \end{pmatrix} \quad (9)$$

Since the permutation matrix is orthogonal,  $\mathbf{P} \mathbf{P}^\top = \mathbf{I}$ , the equation  $\mathbf{A} \mathbf{q} = 0$  is equivalent to  $\mathbf{A} \mathbf{P} \mathbf{P}^\top \mathbf{q} = 0$ . By multiplying the equation sidewise from the left by  $\mathbf{P}^\top$  one gets the equation  $\mathbf{P}^\top \mathbf{A} \mathbf{P} \mathbf{P}^\top \mathbf{q} = 0$ , which can also be expressed explicitly as follows:

$$\begin{pmatrix} \mathbf{M} & \mathbf{m} \\ \mathbf{n}^\top & \mathbf{n}^\top \mathbf{M}^{-1} \mathbf{m} \end{pmatrix} \begin{pmatrix} \frac{-\mathbf{M}^{-1} \mathbf{m}}{\sqrt{1 + \|\mathbf{M}^{-1} \mathbf{m}\|^2}} \\ 1 \\ \frac{1}{\sqrt{1 + \|\mathbf{M}^{-1} \mathbf{m}\|^2}} \end{pmatrix} = \begin{pmatrix} 0 \\ 0 \end{pmatrix} \quad (10)$$

Hence we have determined  $\mathbf{q}_A$  up to a permutation:

$$\mathbf{q}_A = \mathbf{P} \begin{pmatrix} \frac{-\mathbf{M}^{-1} \mathbf{m}}{\sqrt{1 + \|\mathbf{M}^{-1} \mathbf{m}\|^2}} \\ 1 \\ \frac{1}{\sqrt{1 + \|\mathbf{M}^{-1} \mathbf{m}\|^2}} \end{pmatrix} \quad (11)$$

Since the matrix  $\mathbf{M}$  is full rank its determinant is non-zero. The determinant is a smooth function with respect to the matrix entries and since the determinant does not vanish, we infer that the inverse  $\mathbf{M}^{-1}$  is a smooth function with respect to the entries of  $\mathbf{M}$ . Hence we can conclude that  $\mathbf{q}_A$  is a smooth function with respect to the entries of  $\mathbf{A}$ .  $\square$

It should be noticed that in the statement of lemma 1 the word locally means that the eigenmode mapping is smooth for any path as long as the path stays on the manifold defined by  $n \times n$  matrices of rank strictly equal to  $n - 1$ . If the path contains points of rank  $n - 2$  or less, then the eigenmode mapping is no longer continuous at these points. Those points of higher rank deficiency will be at the center of our interest throughout this survey. One can easily picture the case of  $2 \times 2$  rank 1 matrices in ones mind close to the origin, which is rank 0. As long as we are in the neighbourhood of the origin but not at the origin, the eigenmode has some definite direction but at the origin the direction of the eigenmode is no longer defined.

The inner product between two eigenmodes form defined as  $(\mathbf{A}, \mathbf{B}) \mapsto \langle \mathbf{q}_A, \mathbf{q}_B \rangle$ , the angle between two eigenmodes form defined as  $(\mathbf{A}, \mathbf{B}) \mapsto \angle(\mathbf{q}_A, \mathbf{q}_B)$  and the error between two eigenmodes form defined as  $(\mathbf{A}, \mathbf{B}) \mapsto 1 - |\langle \mathbf{q}_A, \mathbf{q}_B \rangle|$  are then all locally smooth forms on the criticality manifold by virtue of composition of smooth functions.

### Parametrization of the $\mathcal{M}_1^2$ manifold of symmetric matrices

Consider the open submanifolds  $U_+ := \{\mathbf{A} \in \mathcal{M}_1^2 : a_{11} \geq 0, a_{22} \geq 0\}$  and  $U_- := \{\mathbf{A} \in \mathcal{M}_1^2 : a_{11} \leq 0, a_{22} \leq 0\}$ . Consider also the inclusion map  $\iota : \mathcal{M}_1^2 \rightarrow \mathbb{R}^{2 \times 2}$ . Then define the charts  $(\varphi_+, U_+)$  and  $(\varphi_-, U_-)$  such that

$$(\varphi_+ \circ \iota^{-1}) \left( \begin{array}{c} \frac{a_{11}}{\pm\sqrt{a_{11}a_{22}}} \pm \frac{\sqrt{a_{11}a_{22}}}{a_{22}} \\ \frac{a_{22}}{\pm\sqrt{a_{11}a_{22}}} \pm \frac{\sqrt{a_{11}a_{22}}}{a_{11}} \end{array} \right) = \left( a_{11} + a_{22}, \frac{1}{\sqrt{2}} \arctan \left( \frac{\pm 2\sqrt{a_{11}a_{22}}}{a_{11} - a_{22}} \right) \right) \quad (12a)$$

$$(\varphi_- \circ \iota^{-1}) \left( \begin{array}{c} \frac{a_{11}}{\pm\sqrt{a_{11}a_{22}}} \pm \frac{\sqrt{a_{11}a_{22}}}{a_{22}} \\ \frac{a_{22}}{\pm\sqrt{a_{11}a_{22}}} \pm \frac{\sqrt{a_{11}a_{22}}}{a_{11}} \end{array} \right) = \left( -a_{11} - a_{22}, \frac{1}{\sqrt{2}} \arctan \left( \frac{\pm 2\sqrt{a_{11}a_{22}}}{a_{22} - a_{11}} \right) \right) \quad (12b)$$

and with the inverse of the maps  $\varphi_+$  and  $\varphi_-$  expressed as follows:

$$(\iota \circ \varphi_+^{-1})(r, \theta) = \frac{r}{2} \begin{pmatrix} 1 + \sin \sqrt{2}\theta & \cos \sqrt{2}\theta \\ \cos \sqrt{2}\theta & 1 - \sin \sqrt{2}\theta \end{pmatrix} \quad (13a)$$

$$(\iota \circ \varphi_-^{-1})(r, \theta) = \frac{r}{2} \begin{pmatrix} -1 - \sin \sqrt{2}\theta & \cos \sqrt{2}\theta \\ \cos \sqrt{2}\theta & -1 + \sin \sqrt{2}\theta \end{pmatrix} \quad (13b)$$

It is not difficult to notice that  $\{(\varphi_+, U_+), (\varphi_-, U_-)\}$  defines a smooth atlas of  $\mathcal{M}_1^2$ . There are many other possibilities to parametrize the criticality manifold, but the one proposed has the particular property that each straight line from the range of  $\varphi_{\pm}$  constitutes a geodesic on the manifold  $\mathcal{M}_1^2$ .

### Geodesics on $\mathcal{M}_1^2$

So far we have not defined the metrics on  $\mathcal{M}_1^2$ , but a very natural choice would be the induced metrics from the ambient space given by the Hilbert-Schmidt inner product for linear operators. Therefore we define the metric tensor  $g(X, Y) := \langle (\iota_* \circ X), (\iota_* \circ Y) \rangle_{\text{HS}}$ , where  $\iota_* : \text{T}\mathcal{M}_1^2 \rightarrow \text{T}\mathbb{R}^{2 \times 2}$  denotes the tangent map of  $\iota$  for any  $X$  and  $Y$  elements of the tangent bundle  $\text{T}\mathcal{M}_1^2$ . The tangent space itself can be defined as  $\text{T}_{\mathbf{A}}\mathcal{M}_1^2 := \text{sp}\left\{ \frac{\partial}{\partial r} \Big|_{\mathbf{A}}, \frac{\partial}{\partial \theta} \Big|_{\mathbf{A}} \right\}$ . Considering the chart  $(\varphi_+, U_+)$ , the push forwards of the vectors  $\frac{\partial}{\partial r} \Big|_{\mathbf{A}}$  and  $\frac{\partial}{\partial \theta} \Big|_{\mathbf{A}}$  by the inclusion map are the given by the following expressions:

$$(\iota_* \circ \frac{\partial}{\partial r}) \Big|_{\mathbf{A}} = \frac{1}{2} \begin{pmatrix} 1 + \sin \sqrt{2}\theta & \cos \sqrt{2}\theta \\ \cos \sqrt{2}\theta & 1 - \sin \sqrt{2}\theta \end{pmatrix} \Big|_{\mathbf{A}} \quad (14a)$$

$$(\iota_* \circ \frac{\partial}{\partial \theta}) \Big|_{\mathbf{A}} = \frac{r}{\sqrt{2}} \begin{pmatrix} \cos \sqrt{2}\theta & -\sin \sqrt{2}\theta \\ -\sin \sqrt{2}\theta & -\cos \sqrt{2}\theta \end{pmatrix} \Big|_{\mathbf{A}} \quad (14b)$$

Similar expressions can be derived for the chart  $(\varphi_-, U_-)$  as well. The metric tensor has then a very neat diagonal form:

$$g_{\mathbf{A}} = \begin{pmatrix} 1 & 0 \\ 0 & r^2 \end{pmatrix} \Big|_{\mathbf{A}} \quad (15)$$

Consider a path  $\gamma : I \rightarrow \mathcal{M}_1^2$ , where  $I$  is some open interval of  $\mathbb{R}$ . That path is said to be a geodesic if  $\nabla_{\dot{\gamma}} \dot{\gamma} \Big|_t = 0$  for all  $t \in I$ . The operator  $\nabla : \text{T}\mathcal{M}_1^2 \times \text{T}\mathcal{M}_1^2 \rightarrow \text{T}\mathcal{M}_1^2$  is the affine riemannian connection that can be evaluated locally using the Riemann-Christoffel symbols  $\Gamma_{ij}^k := g^{kl} \Gamma_{lij}$  and  $\Gamma_{lij} := g(\nabla_{\partial_j} \partial_i, \partial_l) = \frac{1}{2}(\partial_i g_{jl} + \partial_j g_{li} - \partial_l g_{ij})$ . If one considers the parametrization given by the expressions (13a) and (13b), one can check that the only non-zero Riemann-Christoffel symbols are  $\Gamma_{r\theta}^{\theta} = 1/r$  and  $\Gamma_{\theta\theta}^r = -r$ .

**Lemma 2** (Geodesics on  $\mathcal{M}_1^2$ ). *Considering the parametrization (13a) and (13b) any straight line between two points  $\varphi_{\pm}(\mathbf{A})$  and  $\varphi_{\pm}(\mathbf{B})$  belonging to  $\varphi_{\pm}(U_{\pm})$  defines a geodesic on  $U_{\pm}$ .*

*Proof.* The proof is given for the chart  $(\varphi_+, U_+)$ . The proof for the chart  $(\varphi_-, U_-)$  is similar. Consider two points  $\varphi_+(\mathbf{A}) = (r_{|A}, \theta_{|A})$  and  $\varphi_+(\mathbf{B}) = (r_{|B}, \theta_{|B})$ . Take a path  $\gamma : I \rightarrow \mathcal{M}_1^2$  defined by  $(\varphi_+ \circ \gamma)(t) := (1-t)\varphi_+(\mathbf{A}) + t\varphi_+(\mathbf{B}) = (\zeta^r(t), \zeta^\theta(t))$ . The local functions  $\zeta^r$  and  $\zeta^\theta$  can be computed and have the following expressions:

$$\zeta^r(t) = \sqrt{(1-t)^2 r_{|A}^2 + t^2 r_{|B}^2 + 2(1-t)t r_{|A} r_{|B} \cos(\theta_{|A} - \theta_{|B})} \quad (16a)$$

$$\zeta^\theta(t) = \arctan \left( \frac{(1-t)r_{|A} \sin \theta_{|A} + t r_{|B} \sin \theta_{|B}}{(1-t)r_{|A} \cos \theta_{|A} + t r_{|B} \cos \theta_{|B}} \right) \quad (16b)$$

Then one has to show that  $\nabla_{\dot{\gamma}} \dot{\gamma}|_t = 0$  holds locally, i.e. that we have  $\ddot{\zeta}^i + \Gamma_{jk}^i \dot{\zeta}^j \dot{\zeta}^k = 0$  for all  $t \in I$ . Considering only the non-vanishing expressions for the Riemann-Christoffel symbols, one can simplify these equations to the following form:

$$\begin{cases} \ddot{\zeta}^r - \zeta^r (\dot{\zeta}^\theta)^2 & = 0 \\ \ddot{\zeta}^\theta + 2 \frac{1}{\zeta^r} (\dot{\zeta}^r \dot{\zeta}^\theta) & = 0 \end{cases} \quad (17)$$

By carrying out the derivations with respect to  $t$  on the expressions in (16a) and (16b) one can notice that these expression fulfill the equations in (17) and hence that the proposed path is a geodesic on  $U_+$ .  $\square$

It should be noticed that lemma 2 is just an application in the linear operator space of a well known result from geometry of surfaces, which is that if a cone or cylinder (both objects with zero gaussian curvature) are “wrapped” with a paper and a “shortest path” is drawn between two points on the cone or cylinder, then the path drawn on the wrapping paper constitutes a straight line if the paper is “unwrapped” and put on a plane surface.

### Expressions for the angle between two eigenmodes

Let us compute the local expression of an eigenmode  $\mathbf{q}|_{\varphi_+(r,\theta)}$  such that the local expression of the eigenproblem is  $(\iota \circ \varphi_+^{-1})(\mathbf{q} \circ \varphi_+)|_{(r,\theta)} = 0$ . One can easily check that the candidate given by

$$\mathbf{q}|_{\varphi_+(r,\theta)} = \frac{1}{\sqrt{2}} \begin{pmatrix} -\sqrt{1 - \sin \sqrt{2}\theta} \\ \sqrt{1 + \sin \sqrt{2}\theta} \end{pmatrix} \quad (18)$$

will do and that additionally that candidate is normalized to 1. Computation of the inner product  $\langle \mathbf{q}|_A, \mathbf{q}|_B \rangle = \langle (\mathbf{q} \circ \varphi_+)(r_{|A}, \theta_{|A}), (\mathbf{q} \circ \varphi_+)(r_{|B}, \theta_{|B}) \rangle$  results in a very neat expression:

$$\langle \mathbf{q}|_A, \mathbf{q}|_B \rangle^2 = \cos^2 \frac{\theta_{|B} - \theta_{|A}}{\sqrt{2}}. \quad (19)$$

Hence one can infer that the relation modulo  $\pi$  between the angle between the eigenmodes  $\mathbf{q}|_A$  and  $\mathbf{q}|_B$  on one hand and the central angle between the points  $\varphi_+(\mathbf{A})$  and  $\varphi_+(\mathbf{B})$  on the other

$$\sqrt{2} \angle(\mathbf{q}|_A, \mathbf{q}|_B) = \angle(\varphi_+(\mathbf{A}), \varphi_+(\mathbf{B})). \quad (20)$$

Equation (20) is a nice relation, but has an important drawback of being dependant on a particular parametrization. Let's now try to make a relation between the eigenmodes and

some intrinsic properties of the corresponding points on the manifold. Considering the domain  $\varphi_+(U_+) \in \mathbb{R}^2$  on which one can define a point  $\varphi_+(\mathbf{P}) =: P$ , one can decompose the vector  $AB$  in a sum of two position vectors  $AB = -OA + OB$  and by taking the norm on both sides of this equation one gets:

$$\|AB\|^2 = \|OA\|^2 + \|OB\|^2 - 2\|OA\|\|OB\|\cos\angle(A, B). \quad (21)$$

Since the affine function  $t \mapsto (1-t)\varphi_+(\mathbf{P}) + t\varphi_+(\mathbf{Q})$  in  $\varphi_+(U_+) \in \mathbb{R}^2$  is a geodesic on  $U_+ \in \mathcal{M}_1^2$ , one can rewrite equation (21) using distances on the manifold by considering the relation  $\|PQ\| = d_{\mathcal{M}}(\mathbf{P}, \mathbf{Q})$ . Thus we have

$$d_{\mathcal{M}}(\mathbf{A}, \mathbf{B})^2 = d_{\mathcal{M}}(\mathbf{O}, \mathbf{A})^2 + d_{\mathcal{M}}(\mathbf{O}, \mathbf{B})^2 - 2d_{\mathcal{M}}(\mathbf{O}, \mathbf{A})d_{\mathcal{M}}(\mathbf{O}, \mathbf{B})\cos\sqrt{2}\angle(\mathbf{q}|_{\mathbf{A}}, \mathbf{q}|_{\mathbf{B}}). \quad (22)$$

Equation (22) relates the angle between the two eigenmodes  $\mathbf{q}|_{\mathbf{A}}$  and  $\mathbf{q}|_{\mathbf{B}}$  to intrinsic properties of the points  $\mathbf{A}$  and  $\mathbf{B}$  represented by distances on the manifold. Hence if we have two points, one from the non-linear eigenproblem  $\mathbf{A}^{\text{NL}}$  and one from the linearized eigenproblem  $\mathbf{A}^{\text{LIN}}$  we can compute the exact value of the *a posteriori* error  $1 - |\langle \mathbf{q}^{\text{NL}}, \mathbf{q}^{\text{LIN}} \rangle|$ . However this is not of much use since usually we do not have the reference point  $\mathbf{A}^{\text{NL}}$  available. Instead we have to think of another strategy in order to compute the *a priori* error.

#### *A priori error on the eigenmode*

In this context the meaning of the word *a priori* should be understood “without the knowledge of the reference solution”. Therefore we assume that we have at our disposal all possible information for the point  $\mathbf{A}$  on the manifold but not for the point  $\mathbf{B}$ . Instead we have to make some assumptions on the distance and relative angle relative to the point  $\mathbf{B}$ . Note  $\epsilon := d_{\mathcal{M}}(\mathbf{A}, \mathbf{B})$  and  $r|_{\mathbf{A}} := d_{\mathcal{M}}(\mathbf{O}, \mathbf{A})$ . Consider the closed ball of radius  $\epsilon$  centered at  $\mathbf{A}$  that we shall note  $B_{\epsilon}(\mathbf{A}) := \{\mathbf{A} \in \mathcal{M}_1^2 : d_{\mathcal{M}}(\mathbf{A}, \mathbf{B}) \leq \epsilon\}$ . The notation  $\partial B_{\epsilon}(\mathbf{A})$  is for the border of the ball  $B_{\epsilon}(\mathbf{A})$ . The idea is to consider an equiprobable distribution of  $\mathbf{B}$  on the border  $\partial B_{\epsilon}(\mathbf{A})$  for some given radius  $\epsilon$  and center point  $\mathbf{A}$ .

Depending on the ratio of the radius  $\epsilon$  to the distance of the centerpoint from the origin, denoted  $r|_{\mathbf{A}}$ , there are two distinct configurations possible, as shown in figure 9. One can then compute the minimum, average and maximum of the error function  $1 - |\langle \mathbf{q}|_{\mathbf{A}}, \mathbf{q}|_{\mathbf{B}} \rangle|$ . Formally we shall denote:

$$E_{\text{sup}}(\epsilon, \mathbf{A}) := \sup_{\mathbf{B} \in B_{\epsilon}(\mathbf{A})} (1 - |\langle \mathbf{q}|_{\mathbf{A}}, \mathbf{q}|_{\mathbf{B}} \rangle|), \quad (23a)$$

$$E_{\text{av}}(\epsilon, \mathbf{A}) := \frac{1}{\int_{\mathbf{B} \in \partial B_{\epsilon}(\mathbf{A})} d(\theta_{\mathbf{B}} - \theta_{\mathbf{A}})} \int_{\mathbf{B} \in \partial B_{\epsilon}(\mathbf{A})} (1 - |\langle \mathbf{q}|_{\mathbf{A}}, \mathbf{q}|_{\mathbf{B}} \rangle|) d(\theta_{\mathbf{B}} - \theta_{\mathbf{A}}), \quad (23b)$$

$$E_{\text{inf}}(\epsilon, \mathbf{A}) := \inf_{\mathbf{B} \in B_{\epsilon}(\mathbf{A})} (1 - |\langle \mathbf{q}|_{\mathbf{A}}, \mathbf{q}|_{\mathbf{B}} \rangle|). \quad (23c)$$

The the expressions for  $E_{\text{sup}}$ ,  $E_{\text{av}}$  and  $E_{\text{inf}}$  have been drawn in the plot (figure 10) Note that  $E_{\text{inf}} \equiv 0$  always, which means, that for any position of the point  $\mathbf{A}$  and no matter how far or near the point  $\mathbf{B}$  lies, there always exists one direction such that the error on the eigenmode is null. Note also that there is a significant increase both in the supremum of the error function  $E_{\text{sup}}$  and the average  $E_{\text{av}}$  if  $\epsilon \geq r|_{\mathbf{A}}$ . The geometrical interpretation of this increase can be stated in the following way: if the origin  $\mathbf{O}$  is included in the ball  $B_{\epsilon}(\mathbf{A})$  then the point  $\mathbf{B}$  has a possible opportunity to hide “on the opposite side” of the

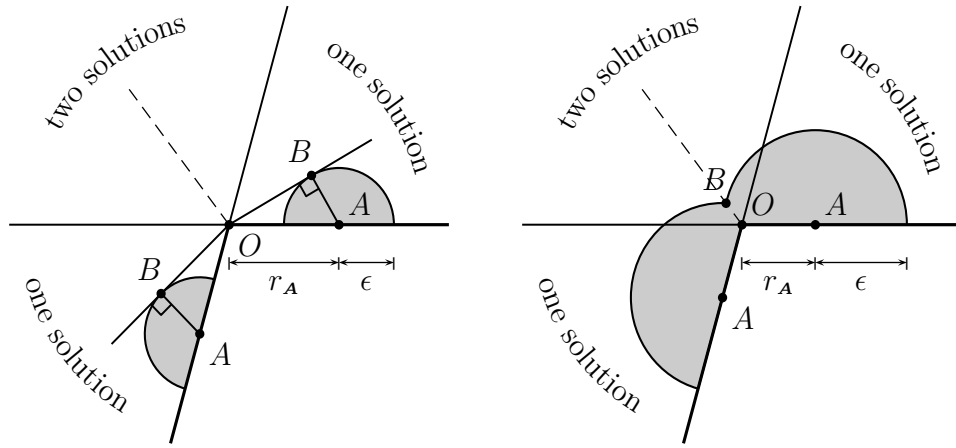


Figure 9. Maximum values for the angle  $\angle AOB$ . On the left for  $\epsilon < r|_A$ . On the right  $\epsilon > r|_A$ .

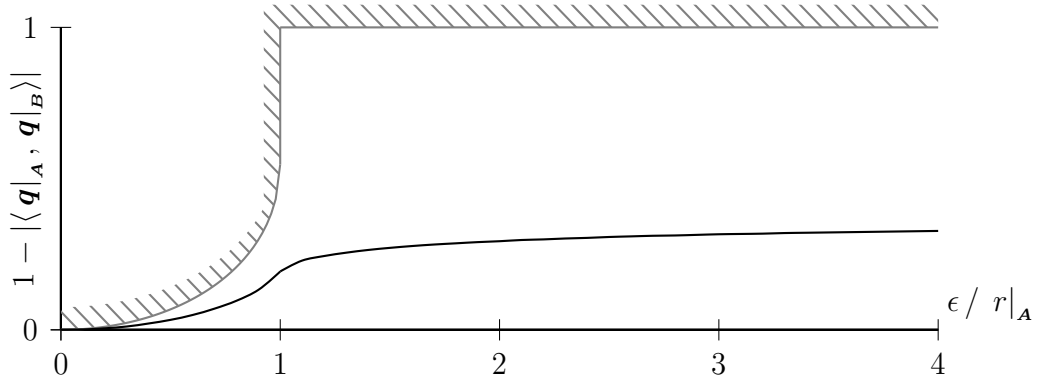


Figure 10. Average and maximum values of the error  $1 - |\langle \mathbf{q}|_A, \mathbf{q}|_B \rangle|$  such that  $B$  is in a ball of radius  $\epsilon$  of center  $A$

manifold, which maximizes the error. On the other hand, if the origin is not included in the ball  $B_\epsilon(\mathbf{A})$ , i.e. if  $\epsilon < r|_A$  then the chances of getting a large error are significantly lower considering the fact that they can be at most of 0.5

### Summary and unsolved questions

It is fairly possible that a reader who has just read this article has some serious doubts about the utility of the methods exposed here, especially regarding the generalization of the claims. Indeed as far we have only shown that for a  $2 \times 2$  symmetric system the error on the eigenmode can possibly be important if the distance on the manifold from the linearized eigenproblem solution point to the reference point is greater than the distance from the linearized solution point to the origin. This notion of an error *possibly* being large obviously brings a probabilistic flavour to the problem, since we can not determine exactly the location of the reference point for a generic problem. However, if we assume some probability distribution for the reference point and consider some statistically important values of the error such that the upper and lower bound and also the average along with standard deviation. Then we have to choose *which* variables are probabilistically distributed and using *what* type of distribution. In this article we showed that the error  $1 - |\langle \mathbf{q}|_A, \mathbf{q}|_B \rangle|$  depends upon two variables: the relative angle  $\theta|_B - \theta|_A$  and the ratio  $\epsilon / r|_A$ . It might be argued that an equiprobable distribution for the relative angle is the

relevant one, since if we consider the set of all possible eigenproblems there is no clear preference for a particular change of direction between the linearized solution and the reference solution. On the other hand the ratio  $\epsilon / r|_{\mathbf{A}}$  depends on the distances between the linearized solution point and the reference point and the distance of the linearized solution point from the origin. Those values could depend on many things, in particular on the degree of non-linearity of the eigenproblem and the position of the jacobian path with respect to the criticality manifold, so for a generic eigenproblem we have not been able, so far, to determine any probability distribution. Therefore have made the choice to leave the ratio  $\epsilon / r|_{\mathbf{A}}$  as an free variable.

What about generalization of the results obtained here to the space of  $n \times n$  eigenproblems? Although we might have some clues about how things are working in higher dimensions, the generalization is really not a straightforward thing to prove. The guess we are making, and which is corroborated by numerous numerical results run on engineering systems, is that submanifolds of higher degree of rank deficiency act as problem areas. If the linearized eigenproblem solution lies close to a point of higher rank deficiency such that for a given  $\epsilon$  the ratio  $\epsilon / r|_{\mathbf{A}}$  becomes large, then we have significantly higher maximum and average values for the error on the eigenmode than if the linearized eigenproblem solution point lied further away.

To summarize, as H. Mang perceptively states in his recent article [17], there is still work to be done in computational stability. Furthermore, as we hope we have been able to show, there are many fields in mathematics, such as differential and algebraic geometry, that so far have not been explored very extensively by engineers. The new tools that we discover today will possibly become the building blocks of some innovative approaches in mechanics tomorrow.

## References

- [1] J.P. Abbott. An efficient algorithm for the determination of certain bifurcation points. *J. of Comp. and Appl. Math.*, 4:19–27, 1974.
- [2] ADINA. *ADINA Theory and Modeling Guide*. ADINA R&D, INC., 2005.
- [3] E.L. Allgover and K. Georg. *Numerical Continuation Methods - An Introduction*. Springer-Verlag, 1990.
- [4] Z.P. Bazant and L. Cedolin. *Stability of Structures*. Oxford University Press, 1991.
- [5] R.D. Cook, D.S. Malkus, M.E. Plesha, and R.J. Witt. *Concepts and Applications of Finite Element Analysis 4th Ed*. John Wiley & Sons, 2002.
- [6] C.J.. Earls. Observations on eigenvalue buckling analysis within a finite element context. In *SSRC Annual Stability Conference*, New Orleans, 2007.
- [7] R.H. Gallagher, R.A. Gellatly, J. Padlog, and R.H. Mallett. A discrete element procedure for thin-shell instability analysis. *AIAA Journal*, 5:138–145, 1967.
- [8] M. Golubitsky and D. Schaeffer. *Singularities and Groups in Bifurcation Theory*. Applied Mathematical Sciences, 17 Springer Verlag, 1985.
- [9] W. Govaerts. *Numerical Methods for Bifurcations of Dynamical Equilibria*. Society for Industrial and Applied Mathematics, Philadelphia, 2000.

- [10] J. Keener and H. Keller. Perturbed bifurcation theory. *Archive for Rational Mechanics and Analysis*, 50:159–175, 1973.
- [11] W.T. Koiter. *Over de stabiliteit van het elastisch evenwicht*. PhD thesis, Technische Hogeschool, Delft, Delft, Netherlands, 1945.
- [12] R. Kouhia and M. Mikkola. Tracing the equilibrium paths beyond simple critical points. *International Journal for Numerical Methods in Engineering*, 28:2933–2941, 1989.
- [13] R. Kouhia and M. Mikkola. Tracing the equilibrium paths beyond compound critical points. *International Journal for Numerical Methods in Engineering*, 46:1049–1074, 1999.
- [14] Y.A. Kuznetsov. *Elements of Applied Bifurcation Theory*. Applied Mathematical Sciences, Springer-Verlag, 1995.
- [15] J.M. Lee. *Introduction to Smooth Manifolds*. Springer, 2003.
- [16] J. Mäkinen, R. Kouhia, A. Fedoroff, and H. Marjamäki. Direct computation of critical equilibrium states for spatial beams and frames. *International Journal for Numerical Methods in Engineering*, 89:135–153, 2011.
- [17] H.A. Mang and X. Jia. Past, present and future research in computational stability of civil engineering structures at vienna university of technology. In *Computational Methods for Engineering Science*, volume 1, pages 25–46. Saxe-Coburg Publications, 2012.
- [18] G. Moore and A. Spence. The calculation of turning points of non-linear equations. *SIAM Journ. of Num. Analysis*, 17:567–576, 1980.
- [19] Gallagher R.H. and Yang H.T.Y. Elastic instability predictions for doubly-curved shells. In *Proceedings of the Second Conference on Matrix Methods in Structural Mechanics*, Wright-Patterson Air Force Base, Ohio, New Jersey, 1968.
- [20] W.C. Rheinboldt. *Numerical Analysis of Parametrized Nonlinear Equations*. Wiley, 1986.
- [21] E. Riks. The incremental solution of some basic problems in elastic stability. In *Technical report NLR TR 74005 U*, The Netherlands, 1974. National Aerospace Laboratory.
- [22] R. Seydel. Numerical calculation of branch points in nonlinear equations. *Numer. Math.*, 33:339–352, 1979.
- [23] R. Seydel. *Practical Bifurcation and Stability Analysis*. Interdisciplinary Applied Mathematics, Springer-Verlag, 1994.
- [24] A. Steinboeck, X. Jia, G. Hoefinger, H. Rubin, and H.A. Mang. Remarkable post-buckling paths analyzed by means of the consistently linearized eigenproblem. *International Journal for Numerical Methods in Engineering*, 76:156–182, 2008.

- [25] R. Thom. *Stabilité structurelle et morphogénèse: essai d'une théorie générale des modèles*. W. A. Benjamin, 1973.
- [26] P. Wriggers and J.C. Simo. A general procedure for the direct computation of turning and bifurcation problems. *International Journal for Numerical Methods in Engineering*, 30:155–176, 1990.

Alexis Fedoroff  
Aalto University, School of Engineering  
Department of Civil and Structural Engineering  
P.O. Box 12100, FI-00076 Aalto  
`alexis.fedoroff@aalto.fi`

Reijo Kouhia  
Tampere University of Technology  
Department of Mechanics and Design  
P.O. Box 589, 33101 Tampere  
`reijo.kouhia@tut.fi`